The Efemp1^{R345W} Macular Dystrophy Mutation Causes Amplified Circadian and Photophobic Responses to Light in Mice

Stewart Thompson,[1–3] Frederick R. Blodi,[2–5] Demelza R. Larson,[3,6,7] Michael G. Anderson,[2,3,6,8] and Steven F. Stasheff[3,4,9–11]

[1]Department of Psychology, New Mexico Tech, Socorro, New Mexico, United States
[2]Ophthalmology and Visual Sciences, University of Iowa, Iowa City, Iowa, United States
[3]Institute for Vision Research, University of Iowa, Iowa City, Iowa, United States
[4]Pediatrics, University of Iowa, Iowa City, Iowa, United States
[5]Ophthalmology and Visual Sciences, University of Louisville, Louisville, Kentucky, United States
[6]Molecular Physiology and Biophysics, University of Iowa, Iowa City, Iowa, United States
[7]Biology Department, College of St. Benedict & St. John's University, Collegeville, Minnesota, United States
[8]VA Center for Prevention and Treatment of Visual Loss, Iowa City, Iowa, United States
[9]Unit on Retinal Neurophysiology, National Eye Institute, Bethesda, Maryland, United States
[10]Center for Neurosciences and Behavioral Medicine, Children's National Medical Center, Washington, DC, United States
[11]George Washington University School of Medicine and Health Sciences, Washington, DC, United States

Correspondence: Stewart Thompson, Department of Psychology, New Mexico Tech, 801 Leroy Place, Socorro, NM 87801, USA; stewart.thompson@nmt.edu.

Submitted: February 19, 2019
Accepted: April 22, 2019

Citation: Thompson S, Blodi FR, Larson DR, Anderson MG, Stasheff SF. The Efemp1^{R345W} macular dystrophy mutation causes amplified circadian and photophobic responses to light in mice. *Invest Ophthalmol Vis Sci.* 2019;60:2110–2117. https://doi.org/10.1167/iovs.19-26881

Purpose. The R345W mutation in *EFEMP1* causes malattia leventinese, an autosomal dominant eye disease with pathogenesis similar to an early-onset age-related macular degeneration. In mice, *Efemp1*^{R345W} does not cause detectable degeneration but small subretinal deposits do accumulate. The purpose of this study was to determine whether there were abnormal responses to light at this presymptomatic stage in *Efemp1*^{R345W} mice.

Methods. Responses to light were assessed by visual water task, circadian phase shifting, and negative masking behavior. The mechanism of abnormal responses was investigated by anterior eye exam, electroretinogram, melanopsin cell quantification, and multielectrode recording of retinal ganglion cell activity.

Results. Visual acuity was not different in *Efemp1*^{R345W} mice. However, amplitudes of circadian phase shifting ($P = 0.016$) and negative masking ($P < 0.0001$) were increased in *Efemp1*^{R345W} mice. This phenotype was not explained by anterior eye defects or amplified outer retina responses. Instead, we identified increased melanopsin-generated responses to light in the ganglion cell layer of the retina ($P < 0.01$).

Conclusions. *Efemp1*^{R345W} increases the sensitivity to light of behavioral responses driven by detection of irradiance. An amplified response to light in melanopsin-expressing intrinsically photosensitive retinal ganglion cells (ipRGCs) is consistent with this phenotype. The major concern with this effect of the malattia leventinese mutation is the potential for abnormal regulation of physiology by light to negatively affect health.

Keywords: circadian rhythms, malattia leventinese, melanopsin, mouse, negative masking

Detection of the amount and timing of light regulates key physiological axes including circadian rhythms, sleep propensity, and widely acting hormones such as pineal melatonin. This function means that eye disease can disrupt the normal regulation of physiology, and potentially have negative health effects. To begin to determine what types of retinal disease affect irradiance measurement, we have screened non–image-forming responses to light in a range of retinal disorder models.[1–6] One selected candidate was the *Efemp1*^{R345W} mouse model of the human disease malattia leventinese.[7]

Epidermal growth factor–containing fibulin-like extracellular matrix protein 1 (EFEMP1) is an extracellular matrix protein that acts as an intermolecular bridge and has tissue remodeling activity.[8,9] An R345W mutation in *EFEMP1* causes the blinding disease malattia leventinese, characterized by progressive accumulation of subretinal deposits typically developing into macular degeneration in mid age.[10] The *EFEMP1*^{R345W} mutation therefore presented a valuable opportunity to advance understanding of macular degeneration, a leading cause of blindness.[11,12] To recapitulate this pathology, *Efemp1*^{R345W} knockin mice were created.[7] However, by 18 months of age subretinal deposits are only microscopic; there is no identifiable retinal degeneration, and the electroretinogram shows that gross outer retinal function is normal. The *Efemp1*^{R345W} mouse therefore appears to represent a presymptomatic stage of macular degeneration.

The initial goal of this study was to determine whether there was an effect of *Efemp1*^{R345W} on responses to light at this presymptomatic stage. We tested visual acuity to identify subtle

deficits not apparent in anatomy or a gross test like the electroretinogram.[13,14] We also tested two responses regulated by detection of irradiance through melanopsin-expressing intrinsically photosensitive retinal ganglion cells (ipRGCs). (1) Detection of major changes in irradiance at dawn and dusk synchronizes the internal circadian clock time with external time cues.[15,16] (2) Detection of high irradiances suppresses activity to reduce predation risk, in a response termed "negative masking."[17] Although negative masking has no obvious correlate in humans, shorter test times support more detailed examination of the properties of a response, with larger sample sizes, than is practical with circadian phase shifts.[18,19]

Given the apparent lack of structure and function defects, we initially hypothesized there would be no effect on function in these tests. Remarkably, *Efemp1*^{R345W} mice had a dramatic increase in amplitude of circadian and negative masking responses to light. We then aimed to identify the source of this amplified response to light. Increased light entering the eye could account for the phenotype so we assessed anterior eye integrity. A plausible inner retina mechanism was also identified by our previous observation of EFEMP1 expression in the ganglion cell layer of the retina, which could directly affect the ipRGCs.[20] We therefore also tested melanopsin-dependent responses to light and the number of melanopsin-expressing cells in the retinal ganglion cell layer.

Methods

All experiments were performed in accordance with the ARVO Statement for the Use of Animals in Ophthalmic and Vision Research and were approved by the University of Iowa Animal Care and Use Review.

Animals and Housing

Generation of *Efemp1*^{R345W} mice on a C57BL/6J background has been previously described.[7] For these studies, *Efemp1*$^{R345W/+}$ and wild-type littermate controls were bred from stock, and genotyped by PCR. Except where indicated, mice were raised and maintained in a repeating cycle of 12 hours dark, 12 hours light at ~19 μWcm^2, with food and water available ad libitum. Experiments were conducted on adult mice between 60 and 180 days old. Separate groups of animals were used for each experiment. Male mice were used for circadian and negative masking tests because wheel running activity is more variable in female mice. For all other tests, similar numbers of male and female mice were used.

Visual Water Task

Visual acuity was tested in *Efemp1*^{R345W} and wild-type littermates (n = 6 each) using the Acumen two-choice discrimination visual water task (Cerebral Mechanics, Lethbridge, Alberta, Canada) according to previously described protocols.[13,14] Mice were trained to criterion on discrimination of a sine wave grating (stationary, vertical, 100% contrast, 0.12 cycles per degree) from an equal total luminance uniform gray stimulus. The threshold for target discrimination was determined, with ≥70% correct performance designated as the threshold for that animal. Comparison was by paired 2-tailed equal variance t-test.

Circadian Photosensitivity

Circadian entrainment and phase shifts to light were measured in male *Efemp1*^{R345W} and wild-type littermates (n = 6 each) as previously described.[1,21,22] Male mice were used for circadian and negative masking tests because wheel running activity is more variable in female mice. Wheel activity was recorded using the ClockLab (Actimetrics, Inc., Evanston, IL, USA). After 10 days of stable entrainment, a 15-minute 0.007-μWcm^2 pulse of fluorescent white light was applied beginning 4 hours after onset of darkness (zeitgeber time 16). Applied irradiance was controlled with neutral-density film (Cinegel; Rosco, Stamford, CT, USA) and confirmed with a PM103 power meter (Macam Photometrics Ltd, Livingston, UK). After the stimuli, mice were maintained in constant darkness for a further 10 days. Amplitude of phase shift was calculated by the difference on the light pulse day between regression lines fitted to pre- and post-stimulus activity onset. Comparison was by 2-tailed t-test.

Negative Masking

Negative masking by bright light was quantified in male *Efemp1*^{R345W} (n = 25) and wild-type littermates (n = 18) according to previously described protocols.[5,17,22] Mice entrained to a daily light/dark cycle were exposed to a 1-hour fluorescent white light stimulus starting 1 hour after lights off on test days (days 2 and 5 of a weekly cycle). Neutral-density film and a power meter were used to provide nine stimulus light levels between 3.3×10^{-7} and 15.4 μWcm^2. Changes in activity over the 1-hour light treatment were calculated as percentage of baseline activity at the corresponding time on the preceding day for each animal. Variable slope sigmoid dose–response curves were fitted in Prism (GraphPad, San Diego, CA, USA) with a fixed minimum at 0%. The irradiance producing a half-maximal response (EC50) and hill slope were calculated from fitted curves. Features of fitted curves were then compared by an F-test of a two-fit comparison in Prism.

Anterior Eye Examination

The anterior chamber of both eyes was examined in awake restrained *Efemp1*^{R345W} and wild-type littermates (n = 5 each) using a slit-lamp SL-D7 (Topcon, Tokyo, Japan).[23] Photographic records were taken at ×25 magnification using a D100 digital camera (Nikon, Tokyo, Japan) with identical camera settings. For transillumination testing, the examination light was directed through the pupil and the capacity to detect light transmitted through the iris maximized by increasing camera exposure time.

Anterior segment anatomy was quantified in *Efemp1*^{R345W} and wild-type littermates (n = 5) by spectral-domain optical coherence tomography (SD-OCT; Bioptigen, Inc., Morrisville, NC, USA).[24] Mice were anesthetized with ketamine:xylazine (100 mg/kg:10 mg/kg), and a tear film was applied (BSS; Alcon Labs, City, TX, USA). A 12-mm telecentric bore was used with reference arm position at 1048, 2.0-mm radial volume scan, 1000 A-scans/B-scan, 100 B-scans/volume, 1 frame/B-scan, and 1 volume. Central corneal thickness (outer epithelium to the endothelium) and anterior chamber depth (corneal endothelium to the anterior lens) were measured using vertical angle-locked B-scan calipers. Comparison was by 2-tailed t-test.

Retinal Ganglion Cell Responses to Light

Light-evoked responses of retinal ganglion cells were recorded from *Efemp1*^{R345W} and C57BL/6J wild-type retinas (n = 6 each) using multielectrode array techniques as previously reported.[25–27] As in other studies, ipRGCs were identified by a sustained response to light in the presence of a pharmacologic cocktail that blocked synaptic input to the retinal ganglion

Investigative Ophthalmology & Visual Science

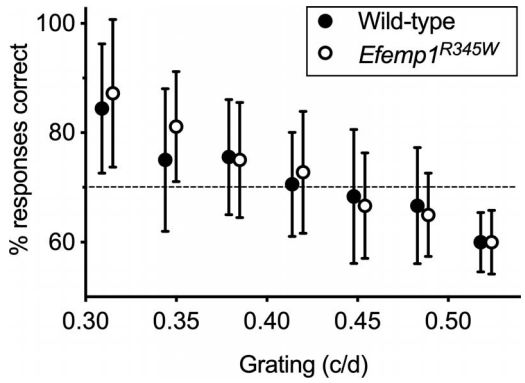

Figure 1. Visual acuity and contrast sensitivity. Performance in the stimulus discrimination–based visual water task is shown for wild-type and *Efemp1*^{R345W} mice ($n = 6$ each, 3 male and 3 female per genotype). The percent of trials in which animals positively identified stimuli with different spatial frequencies versus an equal-luminance control gray screen is shown. Data points are the mean and 95% confidence interval. All data points are offset horizontally to make visualization easier. A correct response rate below 70% was arbitrarily assigned as a fail.

cells. We also tested responses in the presence of the nonspecific gap junction blocker, 18β-glycyrrhetinic acid.[28,29]

Briefly, dark-adapted retinas were placed ganglion cell layer down onto a multielectrode array with 10-μm contacts at 200-μm spacing (Multichannel Systems, Reutlingen, Germany).[30–32] The array was mounted on a Axioplan microscope (Carl Zeiss AG, Oberkochen, Germany) and perfused with 36°C to 37°C oxygenated Ringer medium at 2.5 to 4 mL/min (in mM: 124 NaCl, 2.5 KCl, 2 $CaCl_2$, 2 $MgCl_2$, 1.25 NaH_2PO_2, 26 $NaHCO_3$, and 22 glucose). Preparations were stabilized for 1 hour before testing (Bionic Technologies, Salt Lake City, UT, USA). Rod/cone-generated responses were assessed by full-field 1-second flash stimuli displayed at 5-second intervals and averaged over 10 trials. Melanopsin response assessment was made using a 2-second bright stimulus with synaptic block cocktail added to perfusate (100 μM DL-AP4, 100 μM D-AP5, 20 μM CNQX, 100 μM hexamethonium bromide, 2 μM atropine, 50 μM picrotoxin, and 10 μM strychnine).

Action potential (spike) waveforms accepted for analysis were ≥60 μV in amplitude and ≥1.85 times the root mean square of the background signal. Responses from different cells on the same electrode were distinguished by supervised

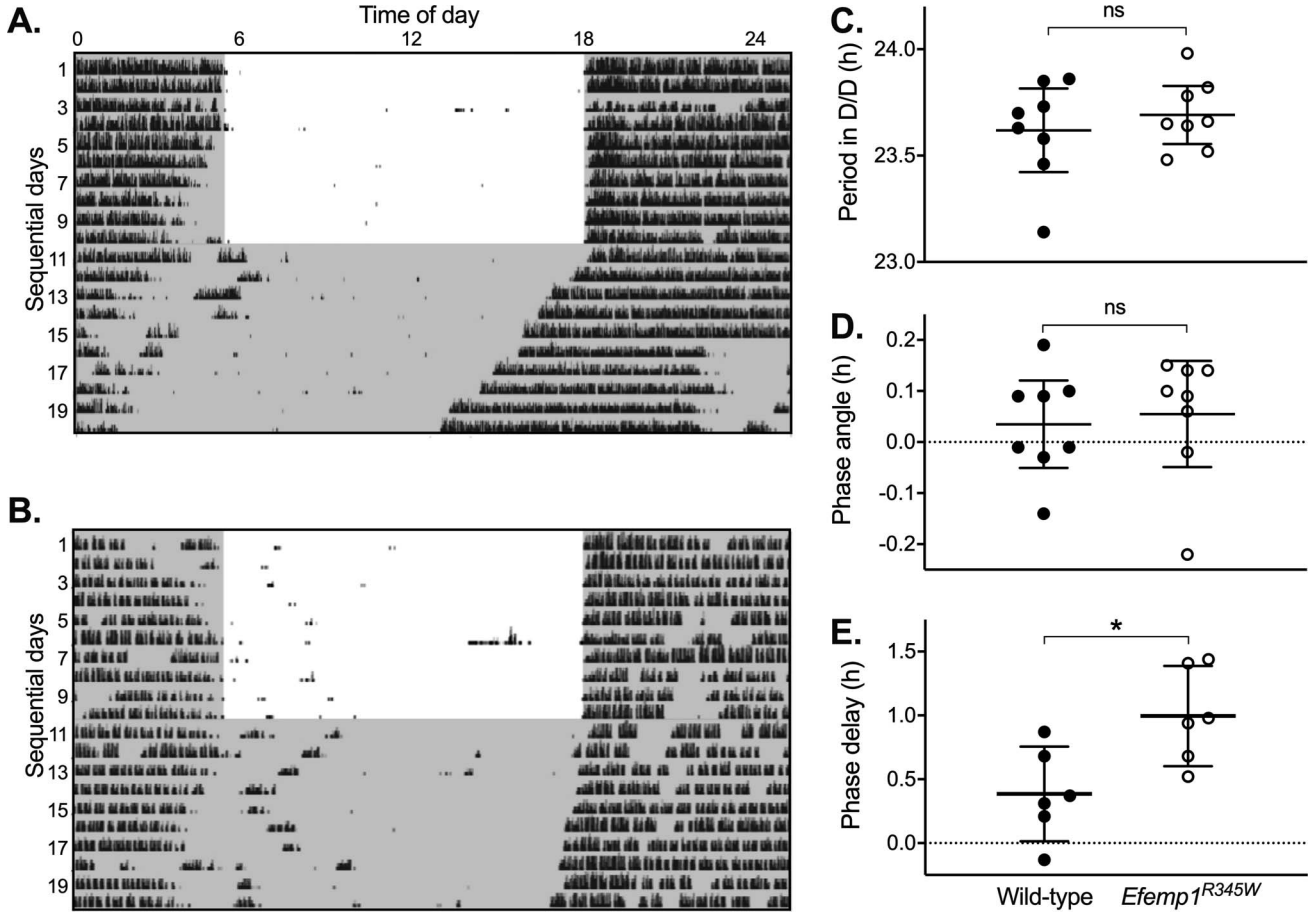

Figure 2. Circadian activity and phase shifting responses to light. Representative records of daily wheel running activity (actograms) are shown for (**A**) wild-type and (**B**) *Efemp1*^{R345W} mice tested under an Aschoff type II protocol. Time of day is shown on the horizontal axis with days shown sequentially from top down. *Black markings* show the timing and amount of running wheel activity, and *gray shading* shows when lights were off. (**C–E**) Mean and 95% confidence interval of derived measures are shown for wild-type and *Efemp1*^{R345W} mice ($n = 8$ each, all male), with significance indicated above data: ns, not significant, $^*P < 0.05$. (**C**) In total darkness (D/D), period between onset of activity each day is slightly less than 24 hours because onset of activity is determined by internal clock time alone. (**D**) In no-light-pulse control experiments, wild-type and *Efemp1*^{R345W} mice were closely entrained to the transition from light to dark: A regression line fitted to activity onset in 24-hour darkness aligns to the lights-off time for the last day in the cycle of light and dark. (**E**) A light pulse applied 4 hours after darkness on the day that mice transitioned to D/D (day 10) induced a delay in onset of activity: A regression line fitted to activity onset for the days after transition to 24-hour darkness aligns to a time after (delay) the lights-off time for the last day in the cycle of light and dark. The timing of the light pulse is apparent in the wild-type actogram (**A**), when there is a light-induced short reduction in activity on day 10, at hour 22 on the actogram or approximately 4 hours after lights off.

Investigative Ophthalmology & Visual Science

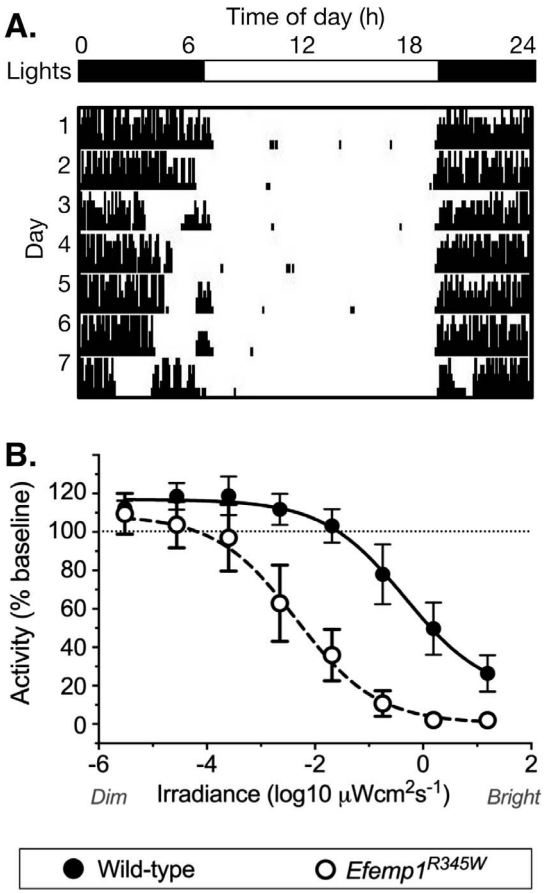

Figure 3. Negative masking. (**A**) A representative wild-type littermate actogram shows how a 1-hour pulse of light applied 1 hour after lights off alters the amount of wheel running in a dose-dependent manner. On day 4, a dim-light pulse causes no suppression of activity. On day 7, a bright-light pulse almost completely suppresses activity for the duration of the stimulus. (**B**) Wheel running activity is shown as a percentage of baseline activity in darkness, plotted by stimulus irradiance for wild-type ($n = 15$, all male) and *Efemp1*^{R345W} mice ($n = 20$, all male). Data points show mean and 95% confidence interval. Fitted dose (irradiance)–response functions are shown.

principal components analysis in PowerNAP, Neuroshare, or Offline Sorter (Plexon Inc., Dallas, TX, USA). Accepted data demonstrated a refractory period of >1 ms (typically 2–5 ms) and did not display recognizable noise patterns (60 Hz, >10 kHz transients, or sinusoidal oscillations). Light-evoked responses were identified by an increase in action potentials starting within the 2 seconds of stimulus on or off. Comparison of the number of cells with a melanopsin-generated response to light was by 2-tailed *t*-test.

Measurement of Melanopsin Ganglion Cell Numbers

The number of melanopsin ganglion cells was compared in *Efemp1*^{R345W} and wild-type littermates ($n = 6$ each, 3 males, 3 females per group).[33] After animals were euthanized, eyes were marked for orientation fixed by immersion in 4% paraformaldehyde–10 mM phosphate-buffered saline, pH 7.4 (PBS) for 4 hours, then transferred to PBS.[34] Retinas were dissected and placed ganglion cell layer upward onto a glass slide, and melanopsin-expressing cells labeled using rabbit anti-mouse melanopsin.[35] Photographs were taken using a BX41 microscope (Olympus, Center Valley, PA, USA) with a SPOT-RT digital camera (Diagnostic Instruments; Burlingame, CA, USA) calibrated using a stage micrometer. Melanopsin-positive cells were counted by defining 1.0-mm^2 areas, 1.0 mm from the optic nerve within each quadrant of the retina, and counting cells that fell within that area.

Results

Visual Function

There was no difference in stimulus discrimination–based visual acuity between wild-type and *Efemp1*^{R345W} mice ($P = 0.61$, Fig. 1).

Circadian Rhythms

Key features of the circadian clock were not significantly different between wild-type and *Efemp1*^{R345W} mice (Fig. 2). *Efemp1*^{R345W} mice showed no significant difference in total activity (mean and SD wheel revolutions per day: wild type = 1064 SD 418, *Efemp1*^{R345W} = 1322 SD 359, $P = 0.29$), and entrained to a daily cycle of light and dark. Endogenous clock-free running period (τ) in constant darkness was slightly shorter than 24 hours (mean and SD: wild type = 23.62 ± 0.24, *Efemp1*^{R345W} = 23.69 ± 0.16; $P = 0.46$), and circadian phase of entrainment (ψ) closely aligned to lights off (wild type = 0.04 ± 0.10 hours, *Efemp1*^{R345W} = 0.06 ± 0.12 hours; $P = 0.77$). However, a phase delay–inducing stimulus applied 4 hours after lights off (zeitgeber time 16) induced a significantly larger phase delay in *Efemp1*^{R345W} mice (mean and SD: wild type = 0.39 ± 0.35 hours, *Efemp1*^{R345W} = 1.00 ± 0.37 hours; $P = 0.016$).

Negative Masking

There was a dramatic 2-log unit increase in sensitivity of the negative masking response to light in *Efemp1*^{R345W} mice (Fig. 3). Analysis of fitted curves shows that this change in dose response is highly significant (EC50 wild-type 2.06 μWcm^2; *Efemp1*^{R345W} 0.016 μWcm^2; *F*-test $P < 0.0001$, $F = 50.94$). However, there was no change in the slope of the curve ($P = 0.97$, $F = 0.0018$).

Outer Retina

Our laboratory repeated electroretinogram assessment and found no difference in *Efemp1*^{R345W} mice for either a-wave or b-wave (see Supplementary Data).

Anterior Eye Integrity

There were no identifiable differences in optics and pigmentation, pupil function, or anatomy of *Efemp1*^{R345W} mice (Fig. 4). On slit-lamp examination, both genotypes had densely pigmented irides, normally shaped pupils, clear corneas, and clear lenses characteristic of the C57BL/6J background.[23] Second, *Efemp1*^{R345W} pupils showed an indistinguishable degree of maximal pupil constriction under the bright examination lighting, suggesting there was no deficit in the iris sphincter muscle or the pupil response to bright light. Third, there was no iris transillumination in wild-type or *Efemp1*^{R345W} mice: A beam of light directed through the pupil reflects back through the pupil and any defects or depigmented areas of the iris. Finally, using SD-OCT there was no detected difference in central corneal thickness ($P = 0.69$) or anterior chamber depth ($P = 0.52$), compared to the average previously measured for C57BL/6J mice.[36]

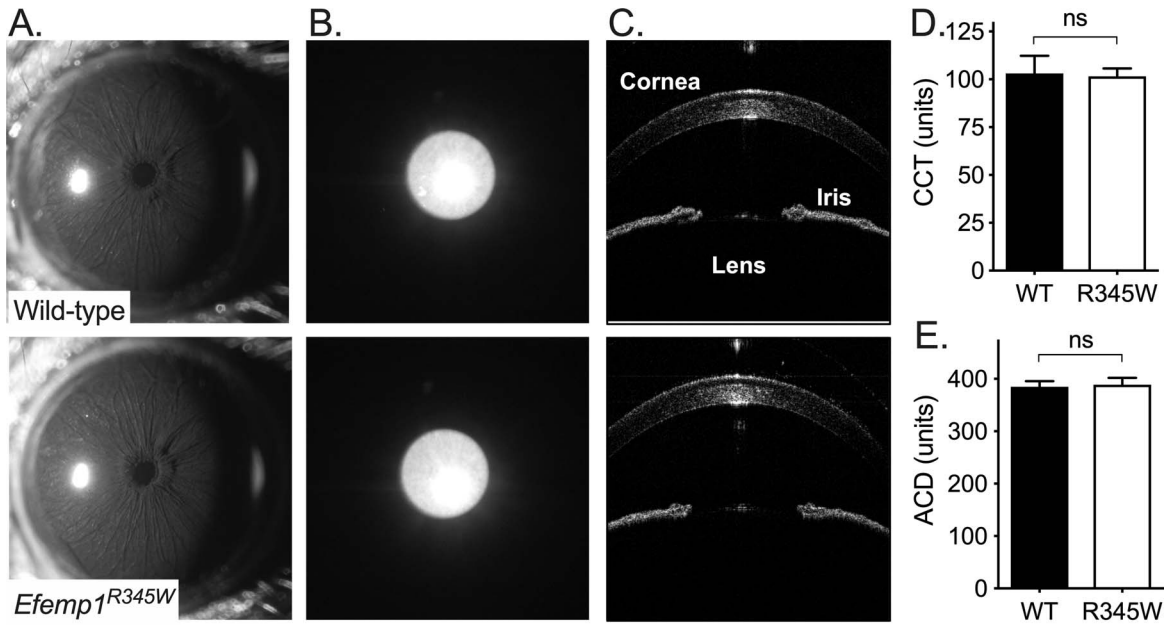

Figure 4. Anterior eye integrity. Example images from wild-type and *Efemp1*^{R345W} mice ($n = 5$ each, 2 males and 3 females per group) are shown for (**A**) slit-lamp examination of the anterior eye under bright light, which shows equivalent pupil constriction; (**B**) iris transillumination, which tests light-blocking capacity of the iris; and (**C**) spectral-domain optical coherence tomography examination of the anterior eye. Mean and 95% confidence interval with significance indicated above data (ns, not significant) are shown for SD-OCT–derived measurements of (**D**) central corneal thickness (CCT) and (**E**) anterior chamber depth (ACD).

Assessing the Effect of *Efemp1*^{R345W} on Melanopsin-Generated Responses to Light

Melanopsin responses had characteristically long latency, and were sustained beyond the stimulus (Fig. 5).[26,27] In wild-type retinas, the number of recorded cells with melanopsin-like responses in synaptic block cocktail was consistent with independent studies using a similar approach (total 45 of 354 cells).[26,27] However, there was a significant increase in the number of recorded cells with melanopsin-like responses in *Efemp1*^{R345W} retinas (total 102 of 386 cells; equal variance unpaired 2-tailed *t*-test $P = 0.008$). Further investigation suggested that this increase in melanopsin-generated responses to light was the result of propagation of ipRGC depolarization to another cell type via gap junctions.

First, in a preliminary assessment, the gap junction blocker 18β-glycyrrhetinic acid halved the number of cells with a melanopsin-generated response to light in two retinas (mean and SD: no gap junction blocker 27.7% ± 8.5%, with gap junction blocker 12.8% ± 2.8%). Although the finding is qualified by a small sample size, this is not significantly different from the percentage of cells with a melanopsin-generated response to light in wild-type mice (Welch's correction unpaired 2-tailed *t*-test $P = 0.98$).

Second, in further analysis of a selection of melanopsin-responsive cells, approximately half of those cells had physiological types inconsistent with ipRGCs when synaptic block was absent.[27] We observed ON-brisk transient (19), ON-OFF (8), OFF (7), and ON-sustained responses (7).[25]

Finally, we found melanopsin-positive soma numbers to be equivalent in wild-type and *Efemp1*^{R345W} mice (mean and SD cell counts from four fields per retina, four retinas per genotype: wild-type 145.8 ± 34.0; *Efemp1*^{R345W} 147.3 ± 26.4; *t*-test $P = 0.95$). This suggested there was no increase in the number of melanopsin cells.

Discussion

The starting position of this study was that *Efemp1*^{R345W} mice might represent a presymptomatic model of macular degeneration, a prevalent blinding disease. Subretinal deposits (drusen) accumulate over decades in patients with malattia leventinese, eventually leading to macular degeneration.[10] In mice, a short lifespan means that *Efemp1*^{R345W} results only in accumulation of limited microscopic subretinal deposits.[7] The limited pathology in mice meant we had a low expectation of any disease phenotype. Remarkably, we identified an increase in sensitivity to light that was present in two distinct non–image-forming responses to light. Further investigation suggested that this phenotype is caused by amplified ipRGC responses to light, a mechanism quite distinct from the outer retina pathology associated with outer retina expression of EFEMP.

Responses to Light

These findings for circadian phase shifting and negative masking were completely unexpected, and dramatic: The change in amplitude of negative masking responses to light was greater than we have observed in 22 different models of retinal diseases or strains of mouse. However, there was no obvious disease mechanism for this effect on irradiance detection–regulated axes. Further, the lack of change in dose–response slope for negative masking is consistent with an unchanged quantum efficiency/photoreceptor input.[1,37] For example, loss of rod and cone photoreceptor input causes a marked steepening of the negative masking response curve.[5] Although qualified in a multivariant system, this did suggest amplification of the signal is downstream of photoreception.

Mechanism

An outer retina mechanism was contraindicated by previous independent reports, as well as our findings on lack of

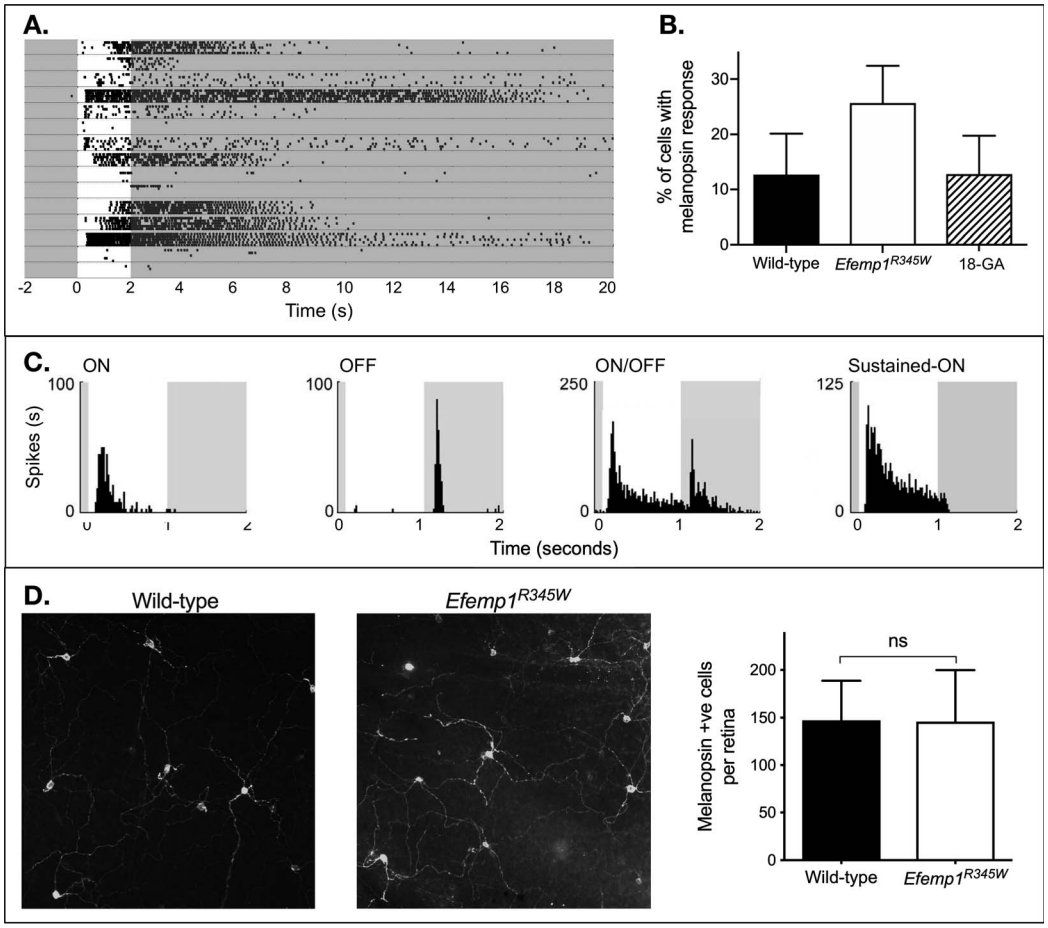

Figure 5. Effects of *Efemp1*^{R345W} on retinal irradiance detection output. (**A**) A representative raster plot showing 15 cells recorded from a multielectrode array recording of the ganglion cell layer of an *Efemp1*^{R345W} retina. Each row shows raster plots of five trials recorded from one cell. *White background*: bright light; *gray*: darkness. Under synaptic block cocktail, some cells show melanopsin-generated responses to light. (**B**) The mean and 95% confidence interval for the percentage of cells with a response to light under synaptic block cocktail are shown for wild-type retinas, *Efemp1*^{R345W} retinas ($n = 6$ each, 3 male and 3 female), and *Efemp1*^{R345W} retinas after addition of the gap junction blocker 18β-glycyrrhetinic acid (18-GA, $n = 2$, both male) to the perfusate. Significance of statistical comparison to wild type is indicated above data: ns, not significant ($^{**}P < 0.01$). (**C**) For cells showing melanopsin-driven responses under synaptic block cocktail that was abolished by 18-GA, physiological responses before synaptic block cocktail was added to perfusate were inconsistent with ipRGCs. Spiking activity is shown in Hertz, with the 1-second full-field flash of light indicated by *white background*. (**D**) Example images at ×20 magnification show anti-melanopsin labeling in wild-type and *Efemp1*^{R345W} retinas, with derived melanopsin cell density counts (mean and 95% confidence interval).

differences in the electroretinogram and visual acuity. Our study also suggested the phenotype was not due to an increase in light entering the eye from an anterior eye defect, such as loss of pigment from the iris or failure of the pupil to constrict in response to light.

An effect at the level of the brain nuclei regulating these responses is possible. For example, an animal model of Smith-Magenis syndrome shows increased effects of light on behavior due to a central hypothalamic mechanism.[38] However, we had previously identified EFEMP1 expression in the ganglion cell layer of the retina, which presented another plausible site of signal amplification.[20] The ganglion cell layer of the retina contains melanopsin-expressing ipRGCs that encode irradiance for circadian and negative masking responses to light.

Multielectrode array recording with pharmacologic blockade of synaptic transmission allowed us to isolate melanopsin-generated responses to light in the retina. Electrophysiology showed a dramatic increase in the number of melanopsin-generated responses in the retina. However, our findings suggested that many of these melanopsin responses were not in ipRGCs: no change in number of melanopsin-positive cells, many cells with melanopsin-generated responses having rod/cone-response properties inconsistent with ipRGCs, and a reduction in number of responding cells with gap junction blocker applied. The gap junction blocker observation is qualified by the number of retinas tested, but our findings are consistent with the demonstrated ipRGC connection to spiking amacrine cells via gap junctions.[39–41] More importantly for this study, our light stimuli did not depolarize the spiking amacrine cells to the spiking threshold in wild-type mice. Therefore, the simplest explanation for our findings is an amplified response to light in the ipRGCs that is sufficient to generate depolarization to spiking threshold in gap junction–connected cells.

The mechanism of *Efemp1*^{R345W} action on ipRGCs has not been determined in this study. Although speculative, EFEMP1 has multiple epidermal growth factor (EGF) domains, and both amacrine and retinal cells express epidermal growth factor receptors (EGFR).[42] This means that an abnormal EGF activity of EFEMP1^{R345W} could alter melanopsin signal transduction or amacrine cell inhibition of the ipRGC response to light.[39,42–44] For example, EGFR can regulate neurite morphology and components in a hypothesized melanopsin phototransduction cascade, including phospholipase C and some TRP chan-

nels.[42,45–47] Our multielectrode array data argue against an acute effect of amacrine cell inhibition of ipRGCs because amacrine cell inhibition of ipRGCs would be abolished in wild-type retinas under synaptic block. However, amacrine cell–mediated effects that persist after synaptic block are still plausible.

Clinical Relevance

Detection of irradiance in humans regulates the circadian clock, sleep, and widely acting hormones such as melatonin. This means that abnormal responses to light could affect health and performance. For example, exposure to artificial light at night is a likely risk factor for breast cancer, with more light at night correlating with increased breast cancer.[48–50] Corroborating this effect, blind women have a lower incidence of breast cancer, with degree of "protection" related to degree of visual function loss: Complete visual function loss reduces incidence by ∼30%.[51,52] It follows that an increased responsiveness to light might exacerbate this negative effect of light at night.

Our study shows that in mice, a mutation causing a retinal disease in humans increases the responsiveness to light in a way that could excerbate negative health effects of artificial light. It is therefore critical that candidate diseases be identified and assessed. Fortunately, suppression of melatonin by light and clinical pupillometry offer practical ways to test the effect of light on irradiance detection axes: Pupillometry is more easily measured but melatonin suppression is likely to be more clinically relevant.[53–56]

Acknowledgments

The authors thank Michael Andrews, Swan Lee, Lisa Liu, Robert Mullins, Megan Riker, Pratibha Singh, Edwin Stone, and Chris Welder for their contributions. *Efemp1^{R345W}* mice were donated by Eric Pierce. Melanopsin antibody was donated by Russell Van Gelder.

Supported by University of Iowa Institute for Vision Research (ST, FRB, SFS), National Institutes of Health P30 EY025580 (DRL), and Veterans Affairs Award #I01 RX001481 (MGA). The contents of this manuscript do not represent the views of the U.S. Department of Veterans Affairs, Department of Defense, or the U.S. Government.

Disclosure: **S. Thompson**, None; **F.R. Blodi**, None; **D.R. Larson**, None; **M.G. Anderson**, None; **S.F. Stasheff**, None

References

1. Hattar S, Lucas RJ, Mrosovsky N, et al. Melanopsin and rod-cone photoreceptive systems account for all major accessory visual functions in mice. *Nature*. 2003;424:76–81.
2. Kuburas A, Thompson S, Artemyev NO, Kardon RH, Russo AF. Photophobia and abnormally sustained pupil responses in a mouse model of bradyopsia. *Invest Ophthalmol Vis Sci*. 2014; 55:6878–6885.
3. Mrosovsky N, Thompson S. Negative and positive masking responses to light in retinal degenerate slow (rds/rds) mice during aging. *Vision Res*. 2008;48:1270–1273.
4. Thompson S, Mullins RF, Philp AR, Stone EM, Mrosovsky N. Divergent phenotypes of vision and accessory visual function in mice with visual cycle dysfunction (Rpe65 rd12) or retinal degeneration (rd/rd). *Invest Ophthalmol Vis Sci*. 2008;49: 2737–2742.
5. Thompson S, Stasheff SF, Hernandez J, et al. Different inner retinal pathways mediate rod-cone input in irradiance detection for the pupillary light reflex and regulation of behavioral state in mice. *Invest Ophthalmol Vis Sci*. 2011;52: 618–623.
6. Thompson S, Whiting REH, Kardon RH, Stone EM, Narfstrom K. Effects of hereditary retinal degeneration due to a CEP290 mutation on the feline pupillary light reflex. *Vet Ophthalmol*. 2010;13:151–157.
7. Fu L, Garland D, Yang Z, et al. The R345W mutation in EFEMP1 is pathogenic and causes AMD-like deposits in mice. *Hum Mol Genet*. 2007;16:2411–2422.
8. de Vega S, Iwamoto T, Yamada Y. Fibulins: multiple roles in matrix structures and tissue functions. *Cell Mol Life Sci*. 2009; 66:1890–1902.
9. Vukovic J, Ruitenberg MJ, Roet K, et al. The glycoprotein fibulin-3 regulates morphology and motility of olfactory ensheathing cells in vitro. *Glia*. 2009;57:424–443.
10. Stone EM, Lotery AJ, Munier FL, et al. A single EFEMP1 mutation associated with both Malattia Leventinese and Doyne honeycomb retinal dystrophy. *Nat Genet*. 1999;22: 199–202.
11. Flaxman SR, Bourne RRA, Resnikoff S, et al. Global causes of blindness and distance vision impairment 1990-2020: a systematic review and meta-analysis. *Lancet Glob. Health*. 2017;5:e1221–e1234.
12. Lin MK, Yang J, Hsu CW, et al. HTRA1, an age-related macular degeneration protease, processes extracellular matrix proteins EFEMP1 and TSP1 [published online ahead of print May 5, 2018]. *Aging Cell*. doi:10.1111/acel.12710.
13. Prusky GT, West PW, Douglas RM. Behavioral assessment of visual acuity in mice and rats. *Vision Res*. 2000;40:2201–2209.
14. Thompson S, Blodi FR, Lee S, et al. Photoreceptor cells with profound structural deficits can support useful vision in mice. *Invest Ophthalmol Vis Sci*. 2014;55:1859–1866.
15. Panda S, Sato TK, Castrucci AM, et al. Melanopsin (Opn4) requirement for normal light-induced circadian phase shifting. *Science*. 2002;298:2213–2216.
16. Ruby NF, Brennan TJ, Xie XM, et al. Role of melanopsin in circadian responses to light. *Science*. 2002;298:2211–2213.
17. Mrosovsky N. Masking: history, definitions, and measurement. *Chronobiol Int*. 1999;16:415–429.
18. Mrosovsky N, Hattar S. Impaired masking responses to light in melanopsin-knockout mice. *Chronobiol Int*. 2003;20:989–999.
19. Thompson S, Foster RG, Stone EM, Sheffield VC, Mrosovsky N. Classical and melanopsin photoreception in irradiance detection: negative masking of locomotor activity by light. *Eur J Neurosci*. 2008;27:1973–1979.
20. Sohn EH, Wang K, Thompson S, et al. Comparison of drusen and modifying genes in autosomal dominant radial drusen and age-related macular degeneration. *Retina*. 2015;35:48–57.
21. Mrosovsky N. Methods of measuring phase shifts: why I continue to use an Aschoff type II procedure despite the skepticism of referees. *Chronobiol Int*. 1996;13:387–392.
22. Thompson S, Philp AR, Stone EM. Visual function testing: a quantifiable visually guided behavior in mice. *Vision Res*. 2008;48:346–352.
23. Anderson MG, Hawes NL, Trantow CM, Chang B, John SW. Iris phenotypes and pigment dispersion caused by genes influencing pigmentation. *Pigment Cell Melanoma Res*. 2008;21: 565–578.
24. Zode GS, Bugge KE, Mohan K, et al. Topical ocular sodium 4-phenylbutyrate rescues glaucoma in a myocilin mouse model of primary open-angle glaucoma. *Invest Ophthalmol Vis Sci*. 2012;53:1557–1565.
25. Stasheff SF, Shankar M, Andrews MP. Developmental time course distinguishes changes in spontaneous and light-evoked

retinal ganglion cell activity in rd1 and rd10 mice. *J Neurophysiol*. 2011;105:3002–3009.

26. Tu DC, Zhang DY, Demas J, et al. Physiologic diversity and development of intrinsically photosensitive retinal ganglion cells. *Neuron*. 2005;48:987–999.
27. Wong KY, Dunn FA, Graham DM, Berson DM. Synaptic influences on rat ganglion-cell photoreceptors. *J Physiol*. 2007;582:279–296.
28. Singer JH, Mirotznik RR, Feller MB. Potentiation of L-type calcium channels reveals nonsynaptic mechanisms that correlate spontaneous activity in the developing mammalian retina. *J Neurosci*. 2001;21:8514–8522.
29. Xia YQ, Nawy S. The gap junction blockers carbenoxolone and 18 beta-glycyrrhetinic acid antagonize cone-driven light responses in the mouse retina. *Vis Neurosci*. 2003;20:429–435.
30. Meister M, Pine J, Baylor DA. Multi-neuronal signals from the retina - acquisition and analysis. *J Neurosci Methods*. 1994;51:95–106.
31. Tian N, Copenhagen DR. Visual deprivation alters development of synaptic function in inner retina after eye opening. *Neuron*. 2001;32:439–449.
32. Segev R, Goodhouse J, Puchalla J, Berry MJ. Recording spikes from a large fraction of the ganglion cells in a retinal patch. *Nat Neurosci*. 2004;7:1155–1162.
33. Wee R, Castrucci AM, Provencio I, Gan L, Van Gelder RN. Loss of photic entrainment and altered free-running circadian rhythms in math5-/- mice. *J Neurosci*. 2002;22:10427–10433.
34. Davis RE, Swiderski RE, Rahmouni K, et al. A knockin mouse model of the Bardet-Biedl syndrome 1 M390R mutation has cilia defects, ventriculomegaly, retinopathy, and obesity. *Proc Natl Acad Sci U S A*. 2007;104:19422–19427.
35. Provencio I, Rollag MD, Castrucci AM. Photoreceptive net in the mammalian retina. This mesh of cells may explain how some blind mice can still tell day from night. *Nature*. 2002;415:493.
36. Lively GD, Jiang B, Hedberg-Buenz A, et al. Genetic dependence of central corneal thickness among inbred strains of mice. *Invest Ophthalmol Vis Sci*. 2010;51:160–171.
37. Peirson SN, Thompson S, Hankins MW, Foster RG. Mammalian photoentrainment: results, methods, and approaches. *Methods Enzymol*. 2005;393:697–726.
38. Diessler S, Kostic C, Arsenijevic Y, Kawasaki A, Franken P. Rai1 frees mice from the repression of active wake behaviors by light. *Elife*. 2017;6:e23292.
39. Reifler AN, Chervenak AP, Dolikian ME, et al. All spiking, sustained ON displaced amacrine cells receive gap-junction input from melanopsin ganglion cells. *Curr Biol*. 2015;25:2763–2773.
40. Muller LP, Do MT, Yau KW, He S, Baldridge WH. Tracer coupling of intrinsically photosensitive retinal ganglion cells to amacrine cells in the mouse retina. *J Comp Neurol*. 2010;518:4813–4824.
41. Sekaran S, Lupi D, Jones SL, et al. Melanopsin-dependent photoreception provides earliest light detection in the mammalian retina. *Curr Biol*. 2005;15:1099–1107.
42. Chen H, Liu B, Neufeld AH. Epidermal growth factor receptor in adult retinal neurons of rat, mouse, and human. *J Comp Neurol*. 2007;500:299–310.
43. Kobayashi N, Kostka G, Garbe JH, et al. A comparative analysis of the fibulin protein family. Biochemical characterization, binding interactions, and tissue localization. *J Biol Chem*. 2007;282:11805–11816.
44. Shimazoe T, Morita M, Ogiwara S, et al. Cholecystokinin-A receptors regulate photic input pathways to the circadian clock. *FASEB J*. 2008;22:1479–1490.
45. Piccolo E, Innominato PF, Mariggio MA, Maffucci T, Iacobelli S, Falasca M. The mechanism involved in the regulation of phospholipase Cgamma1 activity in cell migration. *Oncogene*. 2002;21:6520–6529.
46. Detwiler PB. Phototransduction in retinal ganglion cells. *Yale J Biol Med*. 2018;91:49–52.
47. Odell AF, Scott JL, Van Helden DF. Epidermal growth factor induces tyrosine phosphorylation, membrane insertion, and activation of transient receptor potential channel 4. *J Biol Chem*. 2005;280:37974–37987.
48. James P, Bertrand KA, Hart JE, Schernhammer ES, Tamimi RM, Laden F. Outdoor light at night and breast cancer incidence in the Nurses' Health Study II. *Environ Health Perspect*. 2017;125:087010.
49. Kloog I, Stevens RG, Haim A, Portnov BA. Nighttime light level co-distributes with breast cancer incidence worldwide. *Cancer Causes Control*. 2010;21:2059–2068.
50. Rybnikova N, Haim A, Portnov BA. Artificial light at night (ALAN) and breast cancer incidence worldwide: a revisit of earlier findings with analysis of current trends. *Chronobiol Int*. 2015;32:757–773.
51. Flynn-Evans EE, Stevens RG, Tabandeh H, Schernhammer ES, Lockley SW. Total visual blindness is protective against breast cancer. *Cancer Causes Control*. 2009;20:1753–1756.
52. Pukkala E, Ojamo M, Rudanko SL, Stevens RG, Verkasalo PK. Does incidence of breast cancer and prostate cancer decrease with increasing degree of visual impairment. *Cancer Causes Control*. 2006;17:573–576.
53. Meltzer E, Sguigna PV, Subei A, et al. Retinal architecture and melanopsin-mediated pupillary response characteristics: a putative pathophysiologic signature for the retino-hypothalamic tract in multiple sclerosis. *JAMA Neurol*. 2017;74:574–582.
54. Park JC, Chen YF, Blair NP, et al. Pupillary responses in non-proliferative diabetic retinopathy. *Sci Rep*. 2017;7:44987.
55. Rodgers J, Peirson SN, Hughes S, Hankins MW. Functional characterisation of naturally occurring mutations in human melanopsin. *Cell Mol Life Sci*. 2018;75:3609–3624.
56. Kostic C, Crippa SV, Martin C, et al. Determination of rod and cone influence to the early and late dynamic of the pupillary light response. *Invest Ophthalmol Vis Sci*. 2016;57:2501–2508.

Investigative Ophthalmology & Visual Science